Selective Aerobic Oxidation of Alcohols to Aldehydes over Atomically-dispersed Non-Precious Metal Catalysts

Jiahan Xie, Kehua Yin, Alexey Serov, Kateryna Artyushkova, Hien N. Pham, Xiahan Sang, Raymond R. Unocic, Plamen Atanassov, Abhaya K. Datye and Robert J. Davis*

J. Xie, K. Yin, Prof. R. J. Davis

Department of Chemical Engineering, University of Virginia,

102 Engineers' Way, PO Box 400741, Charlottesville, VA 22904-4741, United States

Phone: 1 - 434 - 924 - 6284

Email: rjd4f@virginia.edu

Dr. A. Serov, Dr. K. Artyushkova, Dr. H. N. Pham, Prof. P. Atanassov, Prof. A. K. Datye

Department of Chemical and Biological Engineering and Center for Micro-engineered Materials, University of New Mexico, Albuquerque, NM 87131, United States

Dr. X. Sang, Dr. R. R. Unocic,

Center for Nanophase Materials Sciences, Oak Ridge National Laboratory, Oak Ridge, TN 37831, United States

Abstract:

Iron atoms dispersed throughout a nitrogen-containing carbon matrix catalyze alcohol oxidation reactions by O_2 in the aqueous phase. The used catalyst can be regenerated by a mild treatment in H_2. An observed kinetic isotope effect indicates β-H elimination is a kinetically-relevant step in the mechanism, which can be accelerated by substituting Fe with Cu.

Abstract:

Materials with atomically-dispersed metal present in a highly porous nitrogen-containing carbon matrix were synthesized by a sacrificial support method and demonstrated to catalyze alcohol oxidation reactions at mild conditions. Benzyl alcohol and 5-(hydroxymethyl)furfural were selectively oxidized to aldehyde products by O_2 in the aqueous phase at 353 K over an Fe-containing catalyst. Individual nitrogen-coordinated iron moieties are proposed to be the active sites for the alcohol oxidation. Rate measurements with deuterated benzyl alcohol revealed a strong kinetic isotope effect, indicating β-H elimination from the alcohol is a kinetically-relevant step in the reaction. Although some deactivation was observed, the original activity was completely regenerated by treatment in H_2 at 573 K. Whereas the rate of 1,6-hexanediol oxidation was substantially slower than that of benzyl alcohol oxidation, addition of 2,2,6,6-tetramethyl-1-piperidinyloxy as a co-catalyst improved the rate of 1,6-hexanediol oxidation by more than an order of magnitude. The rate of benzyl alcohol oxidation was improved when Fe was substituted by other non-precious metals, such as Cr, Co, Ni and Cu. The higher rate of oxidation observed over the Cu catalyst was attributed to faster β-H elimination as the kinetic isotope effect with deuterated benzyl alcohol was much weaker than that observed over Fe catalyst.

Precious metal catalysts are widely used in petrochemical refineries, pharmaceutical production facilities and environmental radiation devices.[1] In particular, the aerobic oxidation of biomass-derived alcohols to corresponding aldehydes and acids in the aqueous phase using heterogeneous precious metal catalysts, such as Au, Pt, Pd and Ru, has received growing attention because it offers a green and sustainable route to value-added chemicals.[2,3] The limited annual production and very high price of the metals, however, can be a significant barrier to commercialization of new processes.[4] Therefore, replacement of precious metals with more earth-abundant metals would be quite advantageous.

Recently, non-precious metal catalysts confined in a nitrogen-containing carbon matrix, which were prepared by pyrolysis or a ball milling method, exhibited decent activity in electrochemical reactions[5–10] and organic synthesis.[11–16] For example, the efficient activation of dioxygen has been reported with Fe-containing, nitrogen-doped carbon (Fe-N-C) in the electrochemical O_2 reduction reaction (ORR), with a comparable activity to the well-known Pt ORR catalysts.[8] Alcohol oxidation reactions can also be catalyzed by the Fe-based catalysts, such as Fe-containing polyoxometalates,[17] nano-Fe_2O_3 particles[18,19] and encapsulated or supported Fe complexes,[20–24] but these catalysts often require the addition of peroxides，which is likely the consequence of the poor ability of the catalyst to activate dioxygen. As an Fe-N-C catalyst has previously demonstrated excellent ORR performance, we hypothesized that it might also be a promising catalyst for the aerobic oxidation of alcohols. In fact, Jagadeesh *et al.* has reported the aerobic oxidative nitrification of various alcohols over Fe-N-C and identified aldehydes as intermediates.[25] To the best of our knowledge, however, the exploration of Fe-N-C

and other platinum group metal-free analogues as potential catalysts for alcohol oxidation in water to produce aldehyde or acid products has not been reported and the mechanism of alcohol oxidation remains unclear.

In this work, an Fe-N-C catalyst synthesized by pyrolysis of $Fe(NO_3)_3$ and nicarbazin (details provided in the supplementary information) was investigated in the aqueous-phase aerobic alcohol oxidation reaction. The weight loading of Fe was determined to be 1.2 wt% from X-ray photoelectron spectroscopy (XPS) (Table S1) and 1.5 wt% from inductively coupled plasma atomic emission spectroscopy (ICP-AES) (Table S2), respectively. The similar metal loading from XPS (surface-sensitive) and ICP-AES (bulk) indicates a relatively uniform distribution of Fe throughout the catalyst. Although the catalyst has been leached with acid to remove Fe or Fe_3C nanoparticles, some nanoparticles (5 – 30 nm) were still observed (Figure S1a), which has also been observed by others using similar synthesis methods and shown to be covered by a graphitic carbon shell.[12,26] In addition to the coated nanoparticles, the existence of atomically-dispersed Fe was confirmed by aberration-corrected scanning transmission electron microscopy (AC-STEM) (Figure 1a). The extensive characterization including XPS, Mössbauer spectroscopy and *in-situ* X-ray absorption spectroscopy indicates these atomically-dispersed sites exist as nitrogen-coordinated Fe ($Fe\text{-}N_x$), which account for ~90% of the relative Fe content evaluated and are proposed to be the ORR active sites.[9]

The rate of benzyl alcohol oxidation over Fe-N-C under mild conditions (353 K, 1 MPa O_2, aqueous solution) was measured to be 1.7×10^{-7} mol s^{-1} g_{cat}^{-1} (Table 1, Entry 2), which is equivalent to a turnover frequency of 0.00078 s^{-1} based on total Fe atoms. As control

experiments, the conversion of benzyl alcohol was evaluated under identical conditions in the presence of Norit activated carbon and activated-carbon-supported Fe (Fe/C) with similar Fe loading and nanoparticle size compared to Fe-N-C (Figures S1). In addition, metal-free nitrogen-containing carbon (N-C) was evaluated for benzyl alcohol oxidation in the absence and presence of soluble Fe^{3+} ($Fe(NO_3)_3$) (Table S3). The conversion of benzyl alcohol over activated carbon and supported Fe nanoparticles was negligible whereas the reaction rate over N-C (with or without the presence of Fe^{3+} ion) is ~20 % of that observed with the equivalent amount of Fe-N-C. The low observed catalytic activity of N-C, compared with Fe-N-C, is likely related to the nitrogen sites on the carbon, which have been reported to participate in the partial reduction of O_2.[27–29] Considering the molar loading of nitrogen in the carbon matrix is much larger than that of Fe (4.7 mol% of N *versus* 0.4 mol% of Fe[9]) and Fe-N-C is about 500% more active than N-C, we propose that the Fe-N_x sites are the primary active sites for benzyl alcohol oxidation.

The reaction orders with respect to O_2 and benzyl alcohol were evaluated over the range of 0.3 – 1 MPa O_2 and 0.025 – 0.1 M benzyl alcohol. As illustrated in Figures S2a and 2b, the reaction orders were close to zero, indicating the saturated adsorption of O_2 and benzyl alcohol. To further explore the reaction mechanism, the kinetic isotope effect utilizing deuterated alcohol ($C_6H_5CD_2OH$) was evaluated. As summarized in Table 2, a significant kinetic isotope effect of 4.8 was observed, indicating β-H elimination is a kinetically-relevant step during benzyl alcohol oxidation over Fe-N-C. For comparison, the KIE was measured to be 1.8 over commercial carbon-supported Pt catalyst (Pt/C), which is a well-studied material for alcohol oxidation.[30] Moreover, the influence of *tert*-butanol and 1,4-benzoquinone, known scavengers for hydroxyl

and superoxide radicals,[31] on the rate of benzyl alcohol oxidation was examined over Fe-N-C and Pt/C. As revealed in Table S4, the introduction of the radical scavengers did not substantially change the rate of alcohol oxidation over either Fe-N-C or Pt/C. These results suggest that radical intermediates are not involved in the benzyl alcohol oxidation over Fe-N-C.

Slight deactivation was observed after 8 h of reaction. As shown in Table 1, Entries 2 and 7, ~35% of the initial activity of Fe-N-C was lost after recovery from the reactor compared to the fresh catalyst. To investigate the cause of deactivation, the used catalyst was characterized by AC-STEM and ICP-AES. High-resolution electron microscopy (Figure 1b) revealed atomically-dispersed Fe-N_x sites remained on the used catalyst and elemental analysis of the fresh and recovered catalysts confirmed that the Fe loading was unaffected by reaction (Table S2). Moreover, the concentration of Fe in the reaction medium after 8 h was less than 0.03 mM, consistent with less than 2% of available iron being leached into the solution. Indeed, the catalytic activity can be almost fully regenerated by a reductive treatment in H_2 (Table 1, Entries 2, 7, 12). These results suggest that the Fe-N_x sites are stable under the reaction conditions and the deactivation is likely the result of strongly adsorbed species on active sites, which were removed during the H_2 treatment. A similar deactivation behavior was also observed during alcohol oxidation over a Pt catalyst.[32]

The oxidation of other alcohols, including 5-hydroxymethylfurfural (HMF), ethanol, 1,6-hexanediol and glycerol, was also investigated over the Fe-N-C catalyst. As shown in Figure 2, benzyl alcohol and HMF were efficiently and selectively converted to benzyl aldehyde and 2,5-diformylfuran (DFF), respectively. The selectivity to benzyl aldehyde and DFF was 92% and

82% at the conversion of 79% and 49%, respectively. Less than 3% conversion of ethanol, 1,6-hexanediol and glycerol was observed under the same conditions, which is likely the result of either more difficult activation of β-H in the aliphatic alcohols or severe catalyst deactivation.

In an attempt to improve the rate of alcohol oxidation over Fe-N-C, 2,2,6,6-tetramethyl-1-piperidinyloxy (TEMPO) was added to the reaction medium, which has been reported to catalyze the oxidation of both aromatic and aliphatic alcohols when combined with homogeneous first-row transition metal co-catalysts.[33,34] As shown in Table S5, the catalytic amount of additive TEMPO (1 mM) significantly increased the rate of benzyl alcohol oxidation. The conversion of benzyl alcohol after 30 min increased from 2.4 % to 12.2% with the addition of TEMPO. More importantly, the oxidation of 1,6-hexanediol, an aliphatic diol, was significantly promoted by TEMPO, with 6.3% conversion after 30 min, compared to 0.5% conversion without the addition of TEMPO.

A series of M-N-C catalysts containing other metals (M = Cr, Co, Ni, Cu) was also prepared by the same method used to synthesize Fe-N-C and evaluated in the benzyl alcohol oxidation. A related study on the oxidative nitrification of alcohols by Jagadeesh *et al*. revealed Fe and Co catalysts exhibited the best activity and selectivity.[25] As shown in Table 1, Entries 1-5, benzyl alcohol was also efficiently converted over all of the M-N-C catalysts in this work. The activity of these M-N-C (M = Cr, Co, Ni, Cu) catalysts was much greater than that of Fe-N-C, among which Cu-N-C was the most active catalyst with a TOF of 0.034 s^{-1} (~50 times greater than that of Fe-N-C and about one order of magnitude lower than Pt). As shown in Figure 1c, the high-resolution STEM image confirmed the atomic dispersion of Cu, which likely resides in

nitrogen-coordinated sites. Similar to Fe-N-C, the reaction order with respect of O_2 and benzyl alcohol was close to 0 in the range of 1 – 2 MPa O_2 and 0.025 – 0.1 M benzyl alcohol over Cu-N-C (Figures S2c and S2d). However, at lower O_2 pressure (0.3 – 1 MPa), the O_2 reaction order was ~0.7. The higher O_2 reaction order over Cu-N-C versus Fe-N-C is possibly correlated to the observed lower activity of Cu-N-C in ORR as reported by Serov *et al*.[35] Interestingly, a much weaker kinetic isotope effect was observed during oxidation of deuterated benzyl alcohol over Cu-N-C compared to Fe-N-C (2.2 versus 4.9) (Table 2), which might be related to a more facile β-H elimination on the Cu catalyst.

The stability of M-N-C catalysts was also investigated. Similar to the behavior of Fe-N-C, loss of activity was observed over M-N-C (M = Cr, Co, Ni, Cu) after 8 h of benzyl alcohol oxidation (Table 1, Entries 1-10). More specifically, only ~10% of the initial activity was observed with recycled Co-N-C, Ni-N-C and Cu-N-C catalysts. Microscopy revealed that Cu remained atomically dispersed throughout the reaction (Figure 1d) and negligible Cu leaching was observed by ICP-AES (Table S2). In an attempt to regenerate the activity of used M-N-C, H_2 treatment at 573 K was performed on the recovered catalysts. Whereas the majority of catalytic activity was recovered from Cr-N-C, Fe-N-C and Co-N-C, the Ni-N-C and Cu-N-C samples were not efficiently regenerated (Table 1).

This work provides a systematic evaluation of the aqueous-phase aerobic alcohol oxidation at mild temperature over a series of non-precious-metal M-N-C catalysts. Benzyl alcohol and HMF were efficiently and selectively converted to the aldehyde products over the earth-abundant Fe-N-C catalyst with a slight loss of activity that could be fully regenerated by simple H_2

treatment. The rate of aliphatic alcohol oxidation was quite slow over Fe-N-C but can be significantly promoted by adding a catalytic amount of TEMPO. The highest activity for benzyl alcohol oxidation was obtained over Cu-N-C, which is tentatively attributed to a faster β-H elimination step. Mechanistic studies of these systems are currently underway.

Acknowledgement

This work is supported by the Center for Biorenewable Chemicals (CBiRC) supported by NSF under grant No. EEC-0813570 and in part by the DOE-EERE Fuel Cell Technology Program (subcontract to Northeastern University, with PI Sanjeev Mukerjee). A portion of the microscopy research was conducted at the Center for Nanophase Materials Sciences in Oak Ridge National Lab, which is a DOE Office of Science User Facility.

Key Words

Heterogeneous catalyst; Metal-nitrogen-carbon; Selective alcohol oxidation; Aqueous phase; Aerobic;

References

[1] T. Muroi, in *Noble Met.* (Ed.: Y. Su), InTech, **2012**, pp. 301–334.

[2] J. Nie, J. Xie, H. Liu, *J. Catal.* **2013**, *301*, 83–91.

[3] S. E. Davis, M. S. Ide, R. J. Davis, *Green Chem.* **2013**, *15*, 17–45.

[4] P. C. K. Vesborg, T. F. Jaramillo, *RSC Adv.* **2012**, *2*, 7933–7947.

[5] X. Zheng, J. Deng, N. Wang, D. Deng, W. H. Zhang, X. Bao, C. Li, *Angew. Chemie. Int. Ed.* **2014**, *53*, 7023–7027.

[6] X. Cui, J. Xiao, Y. Wu, P. Du, R. Si, H. Yang, H. Tian, J. Li, W. H. Zhang, D. Deng, et al., *Angew. Chemie. Int. Ed.* **2016**, *100190*, 6708–6712.

[7] X. Zou, X. Huang, A. Goswami, R. Silva, B. R. Sathe, E. Mikmeková, T. Asefa, *Angew. Chemie Int. Ed.* **2014**, *53*, 4372–4376.

[8] M. Shao, Q. Chang, J.-P. Dodelet, R. Chenitz, *Chem. Rev.* **2016**, *116*, 3594–365.

[9] A. Serov, K. Artyushkova, E. Niangar, C. Wang, N. Dale, F. Jaouen, M. T. Sougrati, Q. Jia, S. Mukerjee, P. Atanassov, *Nano Energy* **2015**, *16*, 293–300.

[10] J. Wang, H. Wu, D. Gao, S. Miao, G. Wang, X. Bao, *Nano Energy* **2015**, *13*, 387–396.

[11] R. V Jagadeesh, H. Junge, M. Pohl, J. Radnik, A. Brückner, M. Beller, *J. Am. Chem. Soc.* **2013**, *135*, 10776–10782.

[12] X. Cui, Y. Li, S. Bachmann, M. Scalone, A. E. Surkus, K. Junge, C. Topf, M. Beller, *J. Am. Chem. Soc.* **2015**, *137*, 10652–10658.

[13] R. V Jagadeesh, T. Stemmler, A. Surkus, H. Junge, K. Junge, M. Beller, *Nat. Protoc.* **2015**, *10*, 548–557.

[14] I. Matanovic, S. Babanova, A. Perry III, A. Serov, *Phys. Chem. Chem. Phys.* **2015**, *17*, 13235–13244.

[15] R. V. Jagadeesh, A. E. Surkus, H. Junge, M. Pohl, J. Radnik, J. Rabeah, H. Huan, V. Schunemann, A. Bruckner, M. Beller, *Science.* **2013**, *342*, 1073–1076.

[16] D. Deng, X. Chen, L. Yu, X. Wu, Q. Liu, Y. Liu, H. Yang, H. Tian, Y. Hu, P. Du, et al., *Sci. Adv.* **2015**, *1*, e1500462.

[17] M. R. Farsani, B. Yadollahi, *J. Mol. Catal. A Chem.* **2014**, *392*, 8–15.

[18] F. Shi, M. K. Tse, M. M. Pohl, A. Brückner, S. Zhang, M. Beller, *Angew. Chemie. Int. Ed.* **2007**, *46*, 8866–8868.

[19] Y. Gao, D. Ma, G. Hu, P. Zhai, X. Bao, B. Zhu, B. Zhang, D. S. Su, *Angew. Chem. Int. Ed. Engl.* **2011**, *50*, 10236–40.

[20] A. Modak, J. Mondal, A. Bhaumik, *Appl. Catal. A Gen.* **2013**, *459*, 41–51.

[21] A. Fidalgo-Marijuan, G. Barandika, B. Bazán, M. K. Urtiaga, E. S. Larrea, M. Iglesias, L. Lezama, M. I. Arriortua, *Dalt. Trans.* **2015**, *44*, 213–222.

[22] G. Bilis, K. C. Christoforidis, Y. Deligiannakis, M. Louloudi, *Catal. Today* **2010**, *157*, 101–106.

[23] R. Rahimi, S. Z. Ghoreishi, M. G. Dekamin, *Monatshefte für Chemie* **2012**, *143*, 1031–1038.

[24] A. R. Oveisi, K. Zhang, A. Khorramabadi-zad, O. K. Farha, J. T. Hupp, *Sci. Rep.* **2015**, *5*, 10621.

[25] R. V Jagadeesh, H. Junge, M. Beller, *Nat. Commun.* **2014**, *5*, 4123.

[26] Y. Zhu, B. Zhang, X. Liu, D. W. Wang, D. S. Su, *Angew. Chemie. Int. Ed.* **2014**, *53*, 10673–10677.

[27] K. Artyushkova, A. Serov, S. Rojas-Carbonell, P. Atanassov, *J. Phys. Chem. C* **2015**, *119*, 25917–25928.

[28] U. Martinez, J. H. Dumont, E. F. Holby, K. Artyushkova, G. M. Purdy, A. Singh, N. H. Mack, P. Atanassov, D. A. Cullen, K. L. More, et al., *Sci. Adv.* **2016**, *2*, 1–7.

[29] V. V. Strelko, N. T. Kartel, I. N. Dukhno, V. S. Kuts, R. B. Clarkson, B. M. Odintsov, *Surf. Sci.* **2004**, *548*, 281–290.

[30] M. S. Ide, R. J. Davis, *J. Catal.* **2013**, *308*, 50–59.

[31] M. Q. Yang, Y. Zhang, N. Zhang, Z.-R. Tang, Y. J. Xu, *Sci. Rep.* **2013**, *3*, 3314.

[32] M. S. Ide, D. D. Falcone, R. J. Davis, *J. Catal.* **2014**, *311*, 295–305.

[33] J. M. Hoover, B. L. Ryland, S. S. Stahl, *J. Am. Chem. Soc.* **2013**, *135*, 2357–67.

[34] Q. Cao, L. M. Dornan, L. Rogan, N. L. Hughes, M. J. Muldoon, *Chem. Commun.* **2014**, *50*, 4524–43.

[35] A. Serov, M. H. Robson, M. Smolnik, P. Atanassov, *Electrochim. Acta* **2012**, *80*, 213–218.

Tables and Figures

Table 1. Rates of benzyl alcohol oxidation over fresh, used and regenerated M-N-C catalysts[a]

Entry	Catalyst	Treatment[b]	Rate (10^{-8} mol s^{-1} g_{cat}^{-1})	TOF (10^{-3} s^{-1})[c]
1	Cr-N-C	Fresh	84	6.5
2	Fe-N-C	Fresh	17	0.78
3	Co-N-C	Fresh	180	15
4	Ni-N-C	Fresh	64	3.1
5	Cu-N-C	Fresh	204	34
6	Cr-N-C	Used	46	3.6
7	Fe-N-C	Used	11	0.52
8	Co-N-C	Used	21	1.7
9	Ni-N-C	Used	7.3	0.36
10	Cu-N-C	Used	21	3.5
11	Cr-N-C	Regenerated	67	5.2
12	Fe-N-C	Regenerated	19	0.90
13	Co-N-C	Regenerated	133	11
14	Ni-N-C	Regenerated	14	0.70
15	Cu-N-C	Regenerated	31	5.0

a: Reaction conditions: 353 K, 10 mL 0.05 M benzyl alcohol aqueous solution, 0.0400 g Fe-N-C or 0.0130 g M-N-C (M = Cr, Co, Ni, Cu), 1 MPa O_2. Reaction profiles are shown in Figure S3.

b: The used catalysts were recovered after 8 h of benzyl alcohol oxidation reaction, washed and dried; The regenerated catalysts were recovered after 8 h of oxidation reaction, washed, dried and treated in dihydrogen flow at 573 K for 3 h.

c: The turnover frequency (TOF) [mol alcohol converted $(\text{mol metal})^{-1}$ s^{-1}] was derived from the initial rate calculated from conversion after 30 min of reaction, which was below 10% in all cases (Figure S3).

Table 2. Kinetics isotope effect and orders of reaction for benzyl alcohol oxidation

Catalyst	TOF_D (10^{-3} s^{-1})[a]	TOF_H/TOF_D	n_{O_2}[b]		$n_{benzyl\ alcohol}$[c]
			0.3 – 1 MPa	1 – 2 MPa	
Fe-N-C	0.16	4.9	0	0	0
Cu-N-C	16	2.2	0.7	0	0

a: The turnover frequency (TOF) [mol alcohol converted (mol metal)$^{-1}$ s^{-1}] was derived from the initial rate calculated from conversion after 30 min of reaction, which was below 10% in all cases. Reaction conditions: 353 K, 10 mL 0.05 M deuterated benzyl alcohol ($C_6H_5CD_2OH$) aqueous solution, 0.0400 g Fe-N-C or 0.0130 g M-N-C (M = Cr, Co, Ni, Cu), 1 MPa O_2.

b: Reaction conditions: 353 K, 10 mL 0.05 M benzyl alcohol aqueous solution, 0.0400 g Fe-N-C or 0.0130 g Cu-N-C, 0.3 – 2 MPa O_2.

c: 353 K, 10 mL benzyl alcohol aqueous solution (0.025 – 0.1 M), 0.0400 g Fe-N-C or 0.0130 g Cu-N-C, 1 MPa O_2.

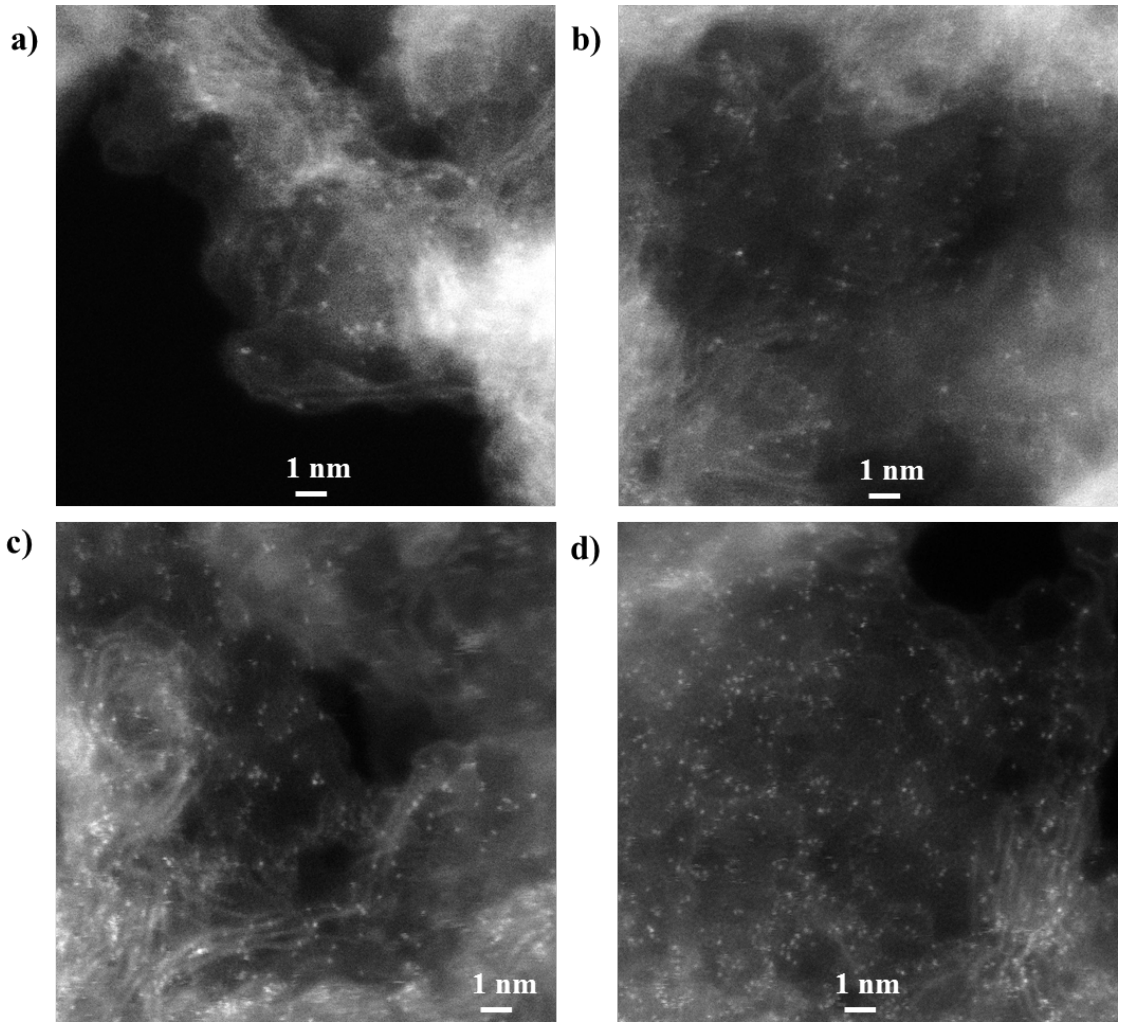

Figure 1. Aberration-corrected STEM images of a) fresh Fe-N-C, b) used Fe-N-C, c) fresh Cu-N-C and d) used Cu-N-C-R. Used catalysts were recovered after 8 h of benzyl alcohol oxidation reaction, washed and dried.

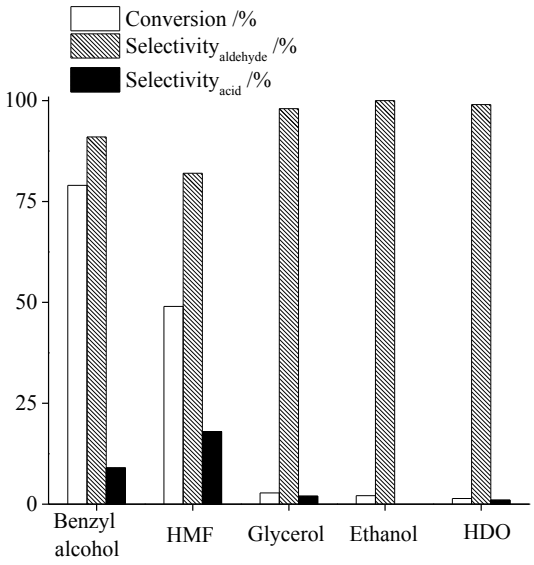

Figure 2. Conversion and product distribution from oxidation of benzyl alcohol, 5-hydroxymethylfurfural (HMF), glycerol and ethanol over Fe-N-C. Reaction conditions: 353 K, 10 mL 0.05 M benzyl alcohol aqueous solution, 0.167 g Fe-N-C, 1 MPa O_2, 8 h reaction time.